

Quantum size effect on ^{67}Zn -NMR measurements of ZnS nanoparticles

H.-Y. Tang,¹ C.-C. Lin,² L.-S. Wang,¹ W.-C. Yang,¹ K.-H. Liao,¹ F.-Y. Li,² and M.-Y. Liao^{2,*}

¹Department of Applied Chemistry, National Chi Nan University, Puli 545, Taiwan

²Department of Chemistry, National Chung Hsing University, Taichung 402, Taiwan

(Received 14 February 2008; published 18 April 2008)

An unusual nuclear magnetic resonance phenomenon is present to demonstrate the quantum size effect of ZnS clusters with its length scale properly estimated within 4 nm from the ^{67}Zn -NMR measurements. Strong quadrupole interaction induced from the quantum size effect is proposed to explain this phenomenon. A simple calculation of the electric field gradient by direct summation over all lattice points was performed to demonstrate this size effect phenomenally, and the result is in good agreement with the experimental observation.

DOI: [10.1103/PhysRevB.77.165420](https://doi.org/10.1103/PhysRevB.77.165420)

PACS number(s): 76.60.Gv, 32.30.Dx, 36.40.Cg

I. INTRODUCTION

Semiconductor clusters of II-VI groups have been the subjects of interest since the last decade due to their unusual physical properties.¹⁻⁷ As the size of a semiconductor cluster approaches the exciton Bohr diameter, its electronic and optical properties, such as band gap or photoluminescent efficiency, vary significantly with their size due to quantum confinement arising from energy quantization.⁸⁻¹⁰ Meanwhile, the thermodynamic properties, such as structure transformation or activation energy, are also affected dramatically due to surface effect arising from the large surface-to-volume ratio.¹¹⁻¹³ Therefore, clear experimental observations of the quantum size effects have been an important issue to demonstrate the discrepancies of optoelectronic and thermodynamic properties for materials from bulk to quantum size regime. For instance, the quantum size effects have been observed by ultraviolet-visible spectroscopy and powder x-ray diffraction for nanometer-scale ZnS clusters.¹⁴⁻¹⁷ The absorption frequency exhibits blueshift and the phase transition temperature is reduced as the average size of the clusters decreases. Nuclear magnetic resonance (NMR) spectroscopy is a powerful tool to probe the electronic structure and environment of atoms in solids, and has been applied to characterize the properties of nanometer-scale clusters.^{18,19} Similar quantum size effects are also demonstrated in nuclei of spin $1/2$ systems either via the Knight shift of small metallic particles or the paramagnetic shift of semiconductor clusters.²⁰⁻²⁴ However, there is no NMR observation to demonstrate the quantum size effect for quadrupole nucleus (spin $I > 1/2$) system yet. Although it is no doubt that the experiments themselves indicate the existence of quantum size effects, there are insufficient results to precisely determine the length scale of quantum size with the NMR measurements.²⁴

In this work, two samples of zinc-blende ZnS nanoparticles from commercial and wet chemical syntheses are characterized by ^{67}Zn -NMR (spin $I=5/2$) and powder x-ray diffraction. The conventional quantum confinement effect is examined by ultraviolet-visible spectroscopy. An unusual NMR phenomenon in ^{67}Zn -NMR measurements of ZnS nanoparticles is found. When the average size of ZnS nanoparticles is beyond 100 nm, an isotropic chemical shift corresponding to the cubic form of ZnS nanoparticles is observed as expected. However, the signal becomes unde-

tectable when the average size of ZnS nanoparticles is within 3 nm. We surmise that this unusual phenomenon is induced from the quantum size effect. Subsequently, as-prepared ZnS nanoparticles are annealed at different temperatures to generate different sizes of nanoparticles for examining this assumption experimentally. Structural information and average particle size are determined along with annealing process, and the length scale of the quantum size for the ZnS nanoparticle is properly estimated within 4 nm. A simple calculation of the electric field gradient by direct sum over all lattice points for the ZnS nanoparticles of different sizes is performed to demonstrate the size effect, which is in good agreement with the experimental observation.

II. EXPERIMENT

Commercial ZnS nanoparticles were purchased from Aldrich chemicals and used without further purification. As-prepared ZnS nanoparticles were synthesized by a chemical precipitation method at room temperature.²⁵⁻²⁸ The annealed ZnS nanoparticle samples were prepared at five different desired temperatures of 300, 400, 500, 600, and 750 °C separately. The annealing process was carried out by heating the as-prepared ZnS nanoparticles at a rate of 3 °C/min under a controlled argon atmosphere until the final desired temperature was reached. The samples were held at each desired temperature for 1 h and then cooled to the room temperature at a rate of 5 °C/min. The structure and absorption information of the ZnS samples were characterized by x-ray diffraction (XRD), UV, and solid-state NMR. Powder x-ray diffraction was taken on a Shimadzu R-7000 diffractometer using $\text{Cu } K\alpha$ radiation operating at a scan rate of 2°/min with 40 kV and 30 mA. Diffuse reflectance spectra were taken on an Ocean Optics S-2000 detector with deuterium lamp and optical fibers. Solid-state NMR experiments were carried by a Varian INOVA 300 MHz spectrometer with a Chemagnetics 7.5 mm magic angle spinning probe at room temperature. The resonance frequency of ^{67}Zn in zinc nitride solution was used as a standard reference. The data were collected using spin echo sequence with signal averaging of 4096 acquisitions and repetition time of 2 s under magic-angle-spinning rate at 5 kHz.

III. RESULTS AND DISCUSSION

On the top of Fig. 1, it shows that the $\theta/2\theta$ diffraction scans for the commercial and as-prepared ZnS nanoparticles.

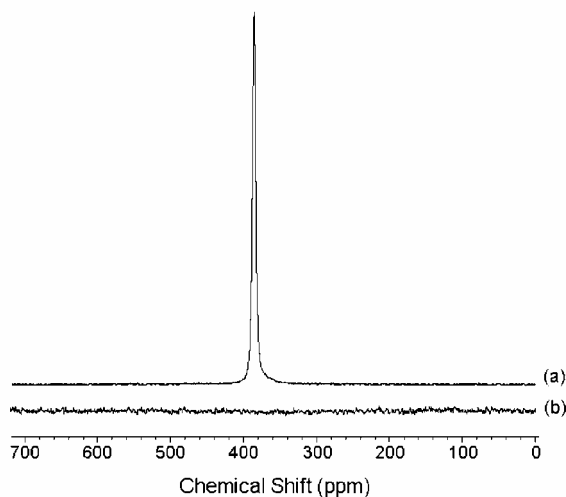
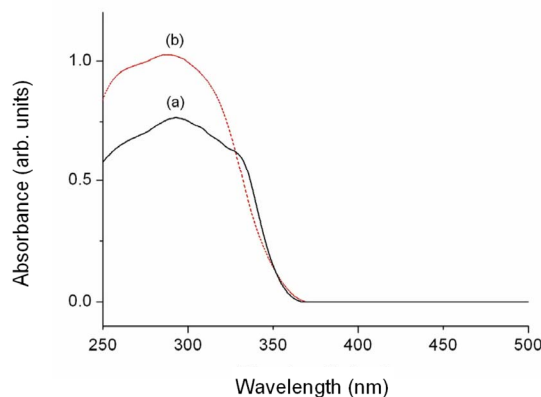
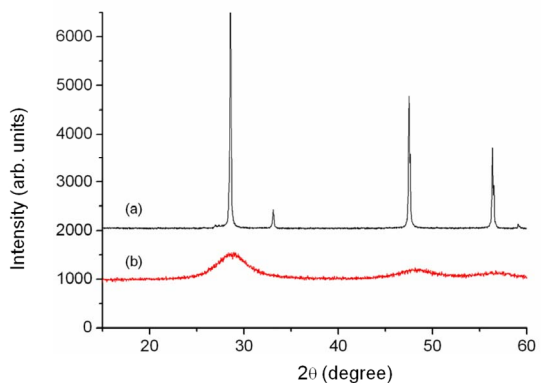


FIG. 1. (Color online) The XRD spectra (top), the diffused reflectance spectra (middle), and the ^{67}Zn -NMR spectra (bottom) of the ZnS clusters (a) from commercial, and (b) as-prepared from wet chemical process.

The XRD patterns for both samples appear at about 28.5° , 47.5° , and 56.3° corresponding to the (111), (220), and (311) planes of zinc-blende structure. However, the linewidth of each peak for the as-prepared ZnS nanoparticles is much broader than that of the commercial product implying that

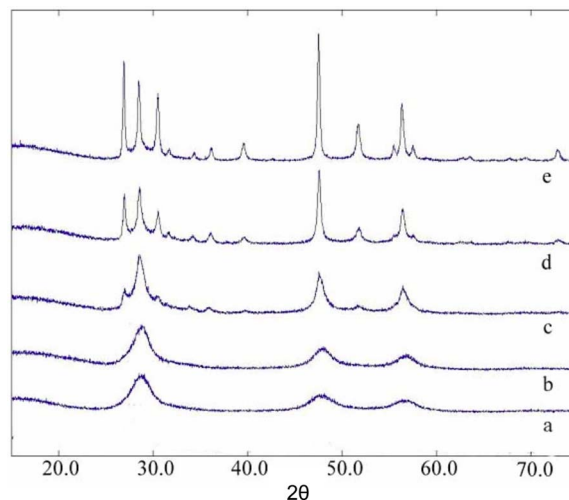


FIG. 2. (Color online) The XRD spectra of the as-prepared ZnS clusters annealed at different temperatures: (a) 300, (b) 400, (c) 500, (d) 600, and (e) 750 $^\circ\text{C}$.

the as-prepared ZnS crystallites are in a smaller average particle size. Scherrer analysis of the XRD peak broadening suggests average sizes of 110 and 3 nm for the commercial and as-prepared ZnS nanoparticles, respectively.²⁹ In the middle of Fig. 1, it shows the diffuse reflectance spectra of the commercial and as-prepared ZnS nanoparticles. Conventional quantum confinement effect is characterized by a blue-shift in the optical absorption. The absorption wavelength is shifted from 340 nm for the commercial ZnS nanoparticles to 300 nm for the as-prepared ZnS nanoparticles. The absorption has a broadband and its wavelength is longer than those measured in the solution state due to the aggregation of the nanoparticles. On the bottom of Fig. 1, it shows the magic-angle-spinning ^{67}Zn -NMR spectra of the commercial and as-prepared ZnS nanoparticles. As it is expected, the commercial ZnS nanoparticles present an isotropic chemical shift of ^{67}Zn -NMR signal at 382 ppm corresponding to the cubic structure.^{30,31} However, there is no detectable ^{67}Zn -NMR signal for the as-prepared ZnS nanoparticles synthesized from the wet chemical process. To confirm this unusual NMR phenomenon, two more experiments have been performed on the as-prepared ZnS nanoparticles separately heated at 60 and 100 $^\circ\text{C}$ for 24 h. Both heated ZnS nanoparticles show similar XRD pattern, but none of them presents any observable ^{67}Zn -NMR signal even with scanning up to 4 MHz range.

It is of interest that the NMR measurements of these ZnS nanoparticles with the average size within the size of exciton Bohr diameter exhibit such a different phenomenon. In order to explicate this size effect and estimate the length scale of the quantum size on the NMR measurements, five samples of the as-prepared ZnS nanoparticles were annealed at five different desired temperatures of 300, 400, 500, 600, and 750 $^\circ\text{C}$ separately. The XRD patterns and the ^{67}Zn -NMR of the as-prepared ZnS nanoparticles annealed at different temperatures are shown in Figs. 2 and 3, respectively. The corresponding average particle size and their structure information during the annealing process are shown in Table I. Most

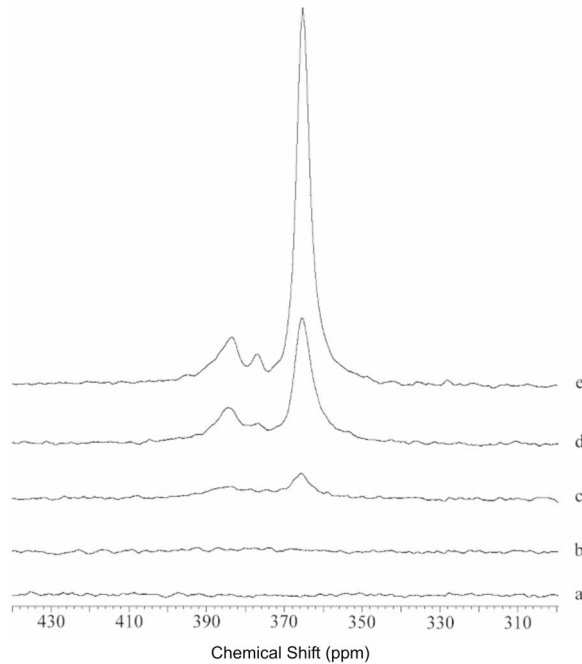


FIG. 3. The ^{67}Zn -NMR spectra of the as-prepared ZnS clusters annealed at different temperatures: (a) 300, (b) 400, (c) 500, (d) 600, and (e) 750 °C.

of the particles remain in cubic form with similar average size within 4 nm when the annealing temperature is below 400 °C, and there is an increase in the average particle size along with phase transformation from zinc blende to wurtzite when the annealing temperature is above 500 °C, as shown in Fig. 2. Generally, the phase transition temperature is around 1020 °C for the commercial ZnS nanoparticles. In our case, the as-prepared ZnS nanoparticles exhibit phase transition from cubic to hexagonal structure around 500 °C. This phenomenon, with a remarkable temperature reduction for structure transformation, can be attributed to the surface effect arising from nanometer-scale particles as expected. However, some of the as-prepared ZnS nanoparticles still remain in the cubic form except the average size is increased to 8 nm after the annealing process, and of course their phase transition occurs at higher temperature. It can be concluded that the structure transformation would occur at any temperature above 500 °C since the annealing process will also increase the average particle size and provide a wide distribution in particle size. As a result, both the average size of the

TABLE I. Structure information of ZnS clusters annealed at different temperatures.

Annealing temp. (°C)	Average size (nm)	XRD structure	^{67}Zn -NMR (ppm)
300	3	Cubic	None
400	4	Cubic	None
500	8	Cubic/hexagonal	382, 377, and 365
600	15	Cubic/hexagonal	382, 377, and 365
750	28	Cubic/hexagonal	382, 377, and 365

particles and the ratio of hexagonal to cubic structure will increase when the annealing temperature is increased from 500 to 750 °C, as shown in Table I.

Figure 2 also shows that the ZnS nanoparticles mainly remain in the cubic form with the average size within 4 nm when the annealing temperature is below 400 °C. It is supposed to observe the chemical shift corresponding to the cubic form in the ^{67}Zn -NMR measurements. However, there is no detectable ^{67}Zn -NMR signal until the annealing temperature reaches 500 °C, as shown in Fig. 3. The ZnS nanoparticles are found in both cubic and hexagonal forms with the average size over 8 nm when the annealing temperature is higher than 500 °C. As expected, the chemical shifts corresponding to both the cubic and hexagonal forms are observed in the ^{67}Zn -NMR spectra. There are three different Zn sites shown in the ^{67}Zn -NMR spectra of the ZnS nanoparticles. The isotropic chemical shifts of 382 and 377 ppm represent for the cubic structure, and the isotropic chemical shift of 365 ppm represents for the hexagonal structure, respectively.³⁰⁻³² These experimental results confirm the existence of the unusual NMR phenomenon and the quantum size effect on the NMR measurement. We conclude that this unusual NMR phenomenon is caused by the quantum size effect since it is observed within the exciton Bohr diameter of ZnS only, which would possibly induce strong interaction at the nucleus site so that the NMR signal is broadened beyond the detection limit. As long as the average size of the nanoparticles is large enough, the quantum size effect is substantially reduced or even extinguished. As a result, the ^{67}Zn -NMR signals will appear as they are expected. The NMR intensities for both cubic and hexagonal forms are enhanced along with the increase in the average particle size during the annealing process, and the ratio of cubic form to hexagonal form is gradually decreased due to the structure transformation, as they are shown in Figs. 2 and 3.

To explore the insight of the relationship between the particle size and the quadrupolar interaction, point monopole model was applied to estimate the electric field gradient (EFG) at each Zn site since each ZnS nanoparticle can be treated as a three-dimensional array of point charges. The components of the EFG tensors are defined as the second partial spatial derivatives of the classical electrostatic potential evaluated at a given nuclear site. Choosing a Zn nucleus as a reference at the origin of the set of crystalline axes xyz , the EFG components at this Zn nucleus are

$$A_{\alpha\beta}^Q = \frac{\partial^2 V}{\partial\alpha\partial\beta} = \frac{e}{4\pi\epsilon_0} \sum_j \zeta(j) S_{\alpha\beta}^Q(j), \quad (1)$$

where the subscripts α and β denote the x , y , and z axes; $e\zeta(j)$ is the electric charge of the j th nucleus; and

$$S_{\alpha\beta}^Q(j) = \sum_i \frac{3\alpha_i(j)\beta_i(j) - r_i^2(j)\delta_{\alpha\beta}}{r_i^5(j)}, \quad (2)$$

where $x_i(j)$, $y_i(j)$ and $z_i(j)$ are the coordinates of the vector $r_i(j)$ between the j th ion and the reference i th nucleus.³³⁻³⁵ Finally, the EFG tensors are diagonalized to obtain its principal components. To demonstrate this size effect on the ^{67}Zn -NMR measurement of ZnS nanoparticles, a series of

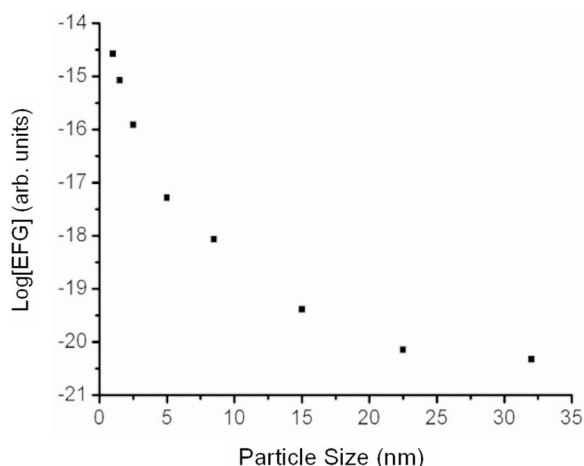


FIG. 4. The calculated electric field gradient at the center of the spherical zinc-blende ZnS clusters of different sizes.

three-dimensional lattices of point charges were generated from the x-ray structure³⁶ to represent different sizes of zinc-blende ZnS spherical nanoparticles. The electric field gradient of each Zn atom within each ZnS nanoparticle, which can be correlated to the size of the quadrupole interaction, is calculated by direct sum over all lattice points. The calculated electric field gradient of Zn site at the center of the zinc-blende ZnS spherical nanoparticle for each size is summarized and shown in Fig. 4. The calculation shows that the electric field gradient around the Zn nucleus at the center of the ZnS nanoparticle will be reduced more than 3 orders magnitude when the average particle size increases from 3 to 15 nm, and will converge when the average particle size is over 30 nm. This result reveals not only the possibility of the existence of strong quadrupolar interaction when the average particle size is within the quantum size region but also

the convergence of the electric field gradient when the average particle size is large enough, which is in good agreement with the experimental result as it is shown Fig. 3.

IV. CONCLUSION

In summary, an unusual NMR phenomenon that there is no detectable ⁶⁷Zn-NMR signal when the average particle size of ZnS nanoparticles is within 4 nm, and the NMR signals appear only when the average particle size of ZnS nanoparticles is above 8 nm is observed. This phenomenon is explained that those ZnS nanoparticles with the average size within the size of exciton Bohr diameter exhibit substantial quantum size effect. As a result, the NMR signal is broadened beyond the detection limit. As long as the average size reaches 8 nm, the size effect is reduced and the NMR signals appear. Although the length scale of quantum size is not able to determine precisely due to the distribution of particle size, the results show definitive evidence that quantum size effect on ⁶⁷Zn-NMR measurement of ZnS nanoparticle occurs when the average size is within 4 nm. Furthermore, the electric field gradients of the Zn nuclear sites in different sizes of ZnS nanoparticles are calculated with a point monopole model to demonstrate the size effect on the NMR measurements. It may not be the best method to evaluate the quantum size effect through this point monopole model. However, the approximation phenomenally provides the correlation between the EFG and average particle size, which is in good agreement with the experimental observations.

ACKNOWLEDGMENT

The financial support of the National Science Council of Taiwan under Grant Nos. 94-2113-M-260-007 and 92-2112-M260-001 are gratefully acknowledged.

*FAX: 886-4-22862547; mliao@nchu.edu.tw

¹A. P. Alivisatos, *J. Phys. Chem.* **100**, 13226 (1996).

²D. J. Norris, Al. L. Efros, M. Rosen, and M. G. Bawendi, *Phys. Rev. B* **53**, 16347 (1996).

³A. P. Alivisatos, *Nat. Biotechnol.* **22**, 47 (2004).

⁴A. Fu, C. M. Micheel, J. Cha, H. Chang, H. Yang, and A. P. Alivisatos, *J. Am. Chem. Soc.* **126**, 10832 (2004).

⁵A. R. Clapp, I. L. Medintz, J. M. Mauro, B. R. Fisher, M. G. Bawendi, and H. Mattoussi, *J. Am. Chem. Soc.* **126**, 301 (2004).

⁶Z. Kónya, V. F. Puentes, I. Kiricsi, J. Zhu, J. W. Ager, III, M. K. Ko, H. Frei, A. P. Alivisatos, and G. A. Somorjai, *Chem. Mater.* **15**, 1242 (2003).

⁷S. Kan, T. Mokari, E. Rothenberg, and U. Banin, *Nat. Mater.* **2**, 155 (2003).

⁸V. L. Colvin, A. P. Alivisatos, and J. G. Tobin, *Phys. Rev. Lett.* **66**, 2786 (1991).

⁹M. G. Bawendi, P. J. Carroll, W. L. Wilson, and L. E. Brus, *J. Chem. Phys.* **96**, 946 (1992).

¹⁰H. Fu and A. Zunger, *Phys. Rev. B* **56**, 1496 (1997).

¹¹S. H. Tolbert, A. B. Herhold, L. E. Brus, and A. P. Alivisatos,

Phys. Rev. Lett. **76**, 4384 (1996).

¹²C.-C. Chen, A. B. Herhold, C. S. Johnson, and A. P. Alivisatos, *Science* **276**, 398 (1997).

¹³Y. Volokitin, J. Sinzig, L. J. de Jongh, G. Schmid, M. N. Vargafik, and I. I. Moiseev, *Nature (London)* **384**, 621 (1996).

¹⁴Y. Nakaoka and Y. Nosaka, *Langmuir* **13**, 708 (1997).

¹⁵R. Rossetti, R. Hull, J. M. Gibson, and L. E. Brus, *J. Chem. Phys.* **82**, 552 (1985).

¹⁶A. D. Dinsmore, D. S. Hsu, S. B. Qadri, J. O. Cross, T. A. Kennedy, H. F. Gray, and B. R. Ratna, *J. Appl. Phys.* **88**, 4985 (2000).

¹⁷S. B. Qadri, E. F. Skelton, D. Hsu, A. D. Dinsmore, J. Yang, H. F. Gray, and B. R. Ratna, *Phys. Rev. B* **60**, 9191 (1999).

¹⁸V. Ladizhansky and S. Vega, *J. Phys. Chem. B* **104**, 5237 (2000).

¹⁹F. V. Mikulec, M. Kuno, M. Bennati, D. A. Hall, R. G. Griffin, and M. G. Bawendi, *J. Am. Chem. Soc.* **122**, 2532 (2000).

²⁰C. D. Makowka, C. P. Slichter, and J. H. Sinfelt, *Phys. Rev. B* **31**, 5663 (1985).

²¹J. P. Bucher and J. J. van der Klink, *Phys. Rev. B* **38**, 11038

- (1999).
- ²²F. C. Fritschij, H. B. Brom, L. J. de Jongh, and G. Schmid, *Phys. Rev. Lett.* **82**, 2167 (1999).
- ²³A. M. Thayer, M. L. Steigerwald, T. M. Duncan, and D. C. Douglass, *Phys. Rev. Lett.* **60**, 2673 (1988).
- ²⁴M. Tomaselli, J. L. Yarger, M. Bruchez, Jr., R. H. Havlin, D. deGraw, A. Pines, and A. P. Alivisatos, *J. Chem. Phys.* **110**, 8861 (1999).
- ²⁵S. Chen and W. Liu, *Langmuir* **15**, 8100 (1999).
- ²⁶J. Nanda, S. Sapra, and D. D. Sarma, *Chem. Mater.* **12**, 1018 (2000).
- ²⁷S. W. Lu, B. I. Lee, Z. L. Wang, W. Tong, B. K. Wagner, W. Park, and C. J. Summers, *J. Lumin.* **92**, 73 (2001).
- ²⁸R. Kho, C. L. Torres-Martinez, and R. K. Mehra, *J. Colloid Interface Sci.* **227**, 561 (2000).
- ²⁹R. Jenkins and R. L. Snyder, *Introduction to X-ray Powder Diffractometry* (Wiley, New York, 1996).
- ³⁰T. J. Bastow and S. N. Stuart, *Phys. Status Solidi B* **145**, 719 (1988).
- ³¹G. Wu, *Chem. Phys. Lett.* **298**, 375 (1998).
- ³²M. Haller, W. E. Hertler, O. Lutz, and A. Nolle, *Solid State Commun.* **33**, 1051 (1980).
- ³³W. W. Simmons and C. P. Slichter, *Phys. Rev.* **121**, 1580 (1961).
- ³⁴F. W. de Wette, *Phys. Rev.* **123**, 103 (1961).
- ³⁵E. N. Kaufmann and R. J. Vianden, *Rev. Mod. Phys.* **51**, 161 (1979).
- ³⁶M. Kh. Rabadanov, A. A. Loshmanov, and Yu. V. Shaldin, *Kristallografiya* **42**, 649 (1997).